nature immunology

The E3 ubiquitin ligase Itch is required for the differentiation of follicular helper T cells

Nengming Xiao[1], Danelle Eto[2], Chris Elly[1], Guiying Peng[1], Shane Crotty[2] & Yun-Cai Liu[1]

Follicular helper T cells (T_{FH} cells) are responsible for effective B cell–mediated immunity, and Bcl-6 is a central factor for the differentiation of T_{FH} cells. However, the molecular mechanisms that regulate the induction of T_{FH} cells remain unclear. Here we found that the E3 ubiquitin ligase Itch was essential for the differentiation of T_{FH} cells, germinal center responses and immunoglobulin G (IgG) responses to acute viral infection. Itch acted intrinsically in $CD4^+$ T cells at early stages of T_{FH} cell development. Itch seemed to act upstream of Bcl-6 expression, as Bcl-6 expression was substantially impaired in *Itch*$^{-/-}$ cells, and the differentiation of *Itch*$^{-/-}$ T cells into T_{FH} cells was restored by enforced expression of Bcl-6. Itch associated with the transcription factor Foxo1 and promoted its ubiquitination and degradation. The defective T_{FH} differentiation of *Itch*$^{-/-}$ T cells was rectified by deletion of *Foxo1*. Thus, our results indicate that Itch acts as an essential positive regulator in the differentiation of T_{FH} cells.

During infection, antibody responses are one of the important host-defense mechanisms used to clear invading pathogens. Antibodies produced by B cells mediate the destruction of extracellular microorganisms and prevent the spread of intracellular infectious agents. The activation of naive B cells is triggered by antigen and usually requires follicular helper T cells (T_{FH} cells) for sustained proliferation and differentiation[1,2]. Germinal centers (GCs) are transient structures in the B cell follicles of secondary lymphoid tissues in which B cells undergo somatic hypermutation, affinity maturation and differentiation into memory B cells and long-lived plasma cells[3]. The formation of GCs is controlled by T_{FH} cells, which are required for the initial help provided to B cells as well as for the maintenance of GCs by positive selection of B cells expressing B cell antigen receptors (BCRs) of the highest affinity. T_{FH} cells also regulate the generation of plasma cells and memory B cells. T_{FH} cells localize in the follicles and GCs because their expression of a set of genes encoding migration-related molecules, most notably the chemokine receptor CXCR5, is different from that of other helper T cells.

T_{FH} cells express interleukin 21 (IL-21), IL-4 and the chemokine CXCL13 and are characterized by high expression of surface markers required for cognate T cell–B cell interactions, including CXCR5, the inducible costimulator ICOS, the T cell inhibitory receptor PD-1, the ligand for the costimulatory receptor CD40 and members of the SLAM family of receptors[1]. Three independent groups have identified the transcription repressor Bcl-6, a member of the BTB-POZ ('bric-a-bric, tramtrack, broad complex–poxvirus zinc finger') family of zinc-finger–containing transcription factors, as a master transcription factor for T_{FH} cells[4–6]. These results clearly established T_{FH} cells as a subset distinct from other T_H cell subsets. However, the regulation of the differentiation of T_{FH} cells is only partially characterized. Accumulating evidences suggests that several cytokines, including IL-6 and IL-21, contribute to the differentiation of T_{FH} cells through mechanisms dependent on the transcription factors STAT3 and STAT1 (refs. 7–12). Signaling via ICOS and its ligand is required for Bcl-6 expression and the differentiation of T_{FH} cells[13,14] and is important for the migration of T_{FH} cells[15]. In contrast, signaling via IL-2 potently inhibits the differentiation of T_{FH} cells by mechanisms dependent on the transcription factors STAT5 and Blimp-1 (refs. 16–18). Blimp-1 is a powerful repressor of Bcl-6 expression[4]. However, details of the mechanisms by which Bcl-6 expression is induced and Bcl-6 is regulated are not well understood[19], nor are the interactions between Bcl-6 and other key transcription factors involved in the differentiation of T_{FH} cells, including c-Maf, BATF, IRF4 and others[13,20–22].

The ubiquitination of proteins is a post-translational modification in which a protein substrate is 'tagged' with the 76–amino acid small polypeptide ubiquitin as mono- or poly-ubiquitin chains, an event catalyzed by a cascade of enzymes, including E1, E2 and E3 (ref. 23). The modified proteins can be subjected to proteasomal degradation or endocytosis, or the ubiquitin modification can instead alter protein function, analogous to phosphorylation or acetylation. Ubiquitin ligases are critical regulators of many biological processes[23]. In T cells, ubiquitin ligases control signaling via the T cell antigen receptor[24], anergy[25], differentiation into T helper type 2 (T_H2) cells[26], differentiation into regulatory T cells[27] and other processes. On the basis of the structural features of their E2-binding domain, most E3 ligases can be classified into two families: RING ('really interesting new gene')-type E3 ligases, and HECT ('homologous to the E6-associated protein carboxyl terminus')-type E3 ligases[28]. Itch belongs to the HECT family of E3 ligases. The locus encoding Itch is disrupted by an inversion in mice of the itchy strain, which develop severe immunological and

[1]Division of Cell Biology, La Jolla Institute for Allergy and Immunology, La Jolla, California, USA. [2]Division of Vaccine Discovery, La Jolla Institute for Allergy and Immunology, La Jolla, California, USA. Correspondence should be addressed to S.C. (shane@liai.org) or Y.-C.L. (yuncail@liai.org).

Received 10 March; accepted 30 April; published online 25 May 2014; doi:10.1038/ni.2912

inflammatory disorders and constant itching of the skin[29]. Itch targets the transcription factors JunB and c-Jun for degradation and inhibits the production of T_H2 cell cytokines[26]. In this study, we present evidence of a critical role for Itch in the differentiation of T_{FH} cells. *Itch*-deficient mice underwent a decrease in the abundance of GC B cells and antigen-specific antibody production after viral infection, due to a cell-intrinsic defect in T_{FH} cell differentiation. This defect in T_{FH} cell differentiation was not associated with T_H2 cells and was independent of signaling via IL-2. Enforced expression of Bcl-6 restored the T_{FH} differentiation of *Itch*$^{-/-}$ T cells, which suggested that Itch functioned upstream of Bcl-6. Unexpectedly, the defective T_{FH} cell differentiation was rectified by ablation of the gene encoding the transcription factor Foxo1. We further demonstrated that Itch associated with Foxo1 and promoted its ubiquitination and subsequent degradation. Our data suggest that Itch is essential for inducing the differentiation of T_{FH} cells and humoral immunity by targeting Foxo1 for degradation.

RESULTS

T_{FH} cell differentiation requires Itch

To investigate the role of E3 ubiquitin ligases in T_{FH} cell differentiation and humoral immune responses, we did a small-scale screen of mice deficient in genes encoding E3 ligases known to be expressed in CD4$^+$ T cells, including *Itch*, *Cblb*, *Cbl* and *Wwp2*, in a model of infection with vaccinia virus (VACV)[14]. At day 8 after infection, we analyzed T cell and B cell responses by flow cytometry and measured virus-specific antibody responses by enzyme-linked immunosorbent assay (ELISA). Mice of the itchy strain (called '*Itch*$^{-/-}$ mice' here) exhibited a significantly lower frequency and absolute number of both T_{FH} cells (CXCR5$^+$SLAM^{lo}) and GC T_{FH} cells (CXCR5$^+$PD-1^{hi} or CXCR5$^+$Bcl-6^{hi}) than that of wild-type mice (**Fig. 1a**,**b**). We observed the considerably defective T_{FH} cell phenotype in *Itch*$^{-/-}$ mice but not in mice with other ubiquitin-ligase deficiencies (**Supplementary Fig. 1a–c**), which indicated a selective role for Itch in the differentiation of T_{FH} cells. To further explore such differentiation in *Itch*$^{-/-}$ mice, we isolated activated CD4$^+$ T cells from VACV-infected wild-type and *Itch*$^{-/-}$ mice and analyzed their T_{FH} cell–related gene-expression profiles by real-time quantitative PCR. The expression of T_{FH} cell–related genes, including *Cxcr5*, *Icos*, *Bcl6* and *IL21*, was lower in activated *Itch*$^{-/-}$ CD4$^+$ T cells than in their wild-type counterparts (**Supplementary Fig. 1d**). *Il4* expression was higher in activated *Itch*$^{-/-}$ CD4$^+$ T cells than in their wild-type counterparts (**Supplementary Fig. 1d**), consistent with a published report[26].

Because T_{FH} cells are the main cognate helpers of antiviral B cell responses[4], we next examined GC formation in *Itch*$^{-/-}$ mice after infection with VACV. As expected, we observed a robust abundance of GC B cells in wild-type C57BL/6J (B6) mice after infection with VACV, but the frequency and absolute number of GC B cells were much lower in their *Itch*$^{-/-}$ counterparts after such infection (**Fig. 1c**,**d** and **Supplementary Fig. 1e**). We then assessed differentiation into plasma cells in wild-type and *Itch*$^{-/-}$ mice after infection with VACV. Consistent with the lower abundance of GC B cells, the number of plasma cells was also much lower in *Itch*$^{-/-}$ mice (**Fig. 1c**,**d**). To assess the consequences of the defective T_{FH} cell and GC B cell responses of *Itch*$^{-/-}$ mice, we measured VACV-specific serum concentrations of immunoglobulin G (IgG). VACV-specific IgG concentrations were 57-fold lower the serum of *Itch*$^{-/-}$ mice than in that of wild-type mice (**Fig. 1e** and **Supplementary Fig. 1f**). Collectively, these data suggested that Itch was required for the generation of T_{FH} cells, GC B cells and high-affinity antibodies.

We next investigated whether Itch deficiency affected the production of inflammatory cytokines and type I interferons during acute viral infection, which could possibly result in enhanced clearance of the infecting virus and indirectly diminish the abundance of T_{FH} cells. We collected serum from wild-type and *Itch*$^{-/-}$ mice at days 1, 2 and 8 after infection with VACV and measured the concentration of inflammatory cytokines (for example, IL-6) and type I interferons in the sera. We observed no substantial differences between wild-type mice and *Itch*$^{-/-}$ mice (**Supplementary Fig. 1g** and data not shown). Furthermore, there was no significant difference in viral load in spleens from wild-type and *Itch*$^{-/-}$ mice 4 d after viral infection ($P = 0.87$; **Supplementary Fig. 1h**). These data suggested that any differences between *Itch*$^{-/-}$ mice and wild-type mice in their innate immune responses did not have much influence on the defective differentiation of T_{FH} cells.

Intrinsic regulation of T_{FH} cell differentiation by Itch

Next we investigated whether Itch regulates T_{FH} cell differentiation in T cell–dependent manner. To address this issue, we crossed mice with a *lox*P-flanked *Itch* exon (*Itch*$^{fl/fl}$)[30] with mice carrying a transgene encoding Cre recombinase under the control of the *Cd4* enhancer-promoter (CD4-Cre) to generate mice with T cell–specific (conditional) *Itch* deficiency (Itch-cKO). We then analyzed the T cell and B cell responses of Itch-cKO mice after infection with VACV. Similar to *Itch*$^{-/-}$ mice, Itch-cKO mice had a much lower frequency and absolute number of both T_{FH} cells (CXCR5$^+$SLAM^{lo}) and GC T_{FH} cells (CXCR5$^+$PD-1^{hi} or CXCR5$^+$Bcl-6^{hi}) than did their wild-type counterparts (**Fig. 1f**,**g**). Moreover, the frequency and number of GC B cells were much lower in Itch-cKO mice than in wild-type mice (**Fig. 1h**,**i** and **Supplementary Fig. 1i**). Furthermore, the generation of plasma cells was also significantly lower in Itch-cKO mice than in wild-type mice (**Fig. 1h**,**i**). Finally, VACV-specific IgG concentrations were 41-fold lower in the serum of Itch-cKO mice than in that of wild-type mice (**Fig. 1j** and **Supplementary Fig. 1j**). The similar phenotypes of *Itch*$^{-/-}$ mice and Itch-cKO mice suggested that Itch regulated T_{FH} cell differentiation and humoral immunity in a T cell–intrinsic manner.

Itch in various stages of T_{FH} cell differentiation

T_{FH} cell differentiation is a multistage, multifactorial process[1]. To investigate at what phases Itch regulates such differentiation, we crossed *Itch*$^{-/-}$ mice with SMARTA mice (which have transgenic expression of a T cell antigen receptor specific for the epitope of lymphocytic choriomeningitis virus (LCMV) glycoprotein amino acids 66–77, presented by the major histocompatibility complex (MHC) class II molecule I-A^b) to generate *Itch*$^{-/-}$ SMARTA mice[31]. We isolated naive CD4$^+$ T cells from *Itch*$^{+/+}$ SMARTA mice (called 'wild-type SMARTA mice' here) and *Itch*$^{-/-}$ SMARTA mice and then adoptively transferred them separately into B6 recipient mice, followed by subsequent acute infection of the host mice with LCMV. Although *Itch*$^{-/-}$ SMARTA CD4$^+$ T cells showed normal proliferation (**Supplementary Fig. 2a**), they almost completely failed to differentiate into T_{FH} cells by day 3 after infection, as measured by gating of CXCR5$^+$SLAM^{lo}, CXCR5$^+$PD-1^{hi} or CXCR5$^+$Bcl-6^{hi} cells (**Fig. 2a**,**b**). Moreover, expression of both CXCR5 protein ($P = 0.0012$) and Bcl-6 protein ($P = 0.0046$) was significantly lower in *Itch*$^{-/-}$ SMARTA CD4$^+$ T cells than in wild-type SMARTA CD4$^+$ T cells (**Supplementary Fig. 2b**). Consistent with that, *Itch*$^{-/-}$ SMARTA CD4$^+$ T cells had lower levels of *Cxcr5*, *Bcl6* and *Il21* mRNA and higher levels of *Prdm1* mRNA (which encodes Blimp-1) at day 3 after infection (**Fig. 2c**). These results suggested that the defective T_{FH} differentiation of *Itch*$^{-/-}$ cells was associated with a failure to express Bcl-6 at early time points.

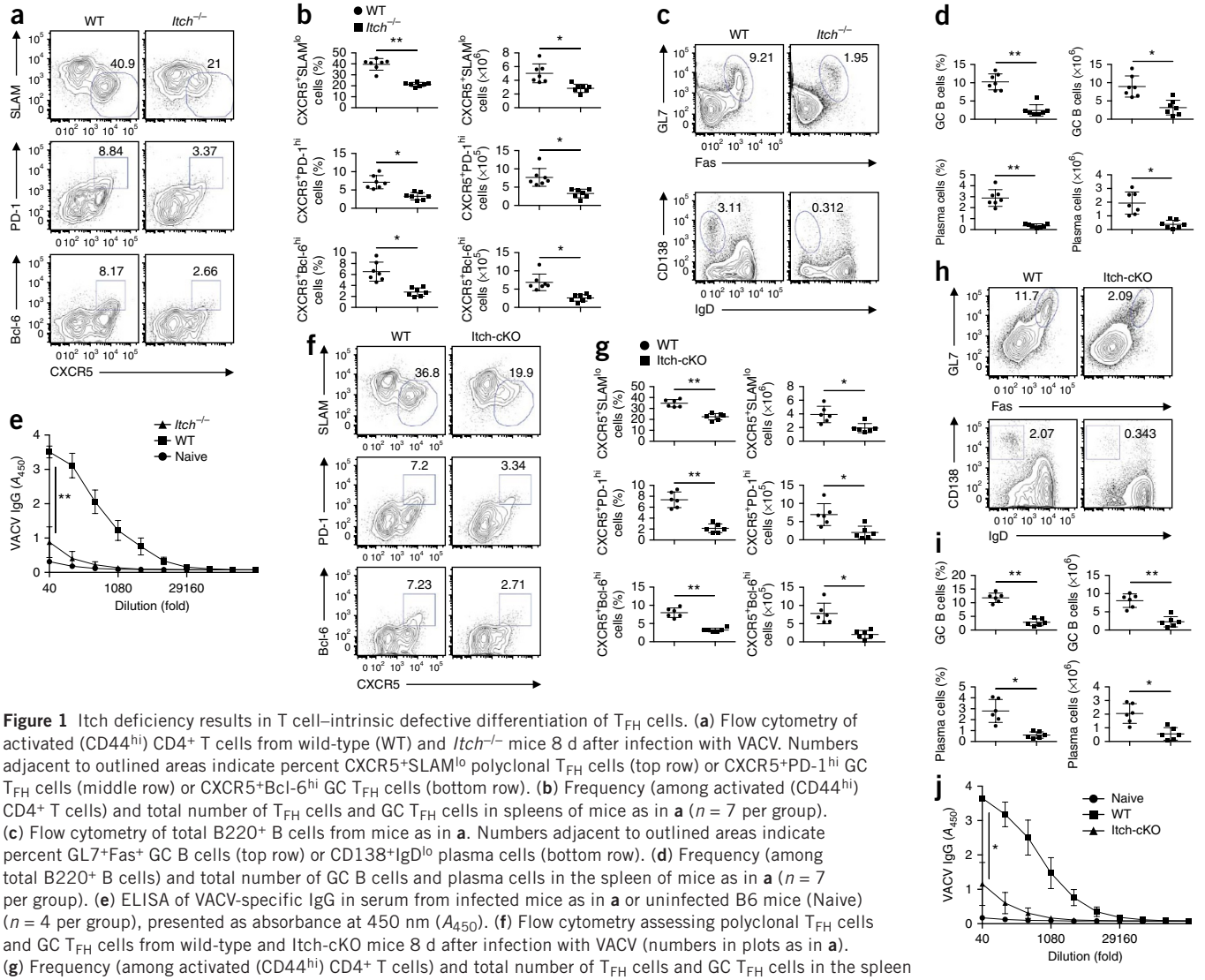

Figure 1 Itch deficiency results in T cell–intrinsic defective differentiation of T_{FH} cells. (**a**) Flow cytometry of activated ($CD44^{hi}$) $CD4^+$ T cells from wild-type (WT) and *Itch*$^{-/-}$ mice 8 d after infection with VACV. Numbers adjacent to outlined areas indicate percent $CXCR5^+SLAM^{lo}$ polyclonal T_{FH} cells (top row) or $CXCR5^+PD\text{-}1^{hi}$ GC T_{FH} cells (middle row) or $CXCR5^+Bcl\text{-}6^{hi}$ GC T_{FH} cells (bottom row). (**b**) Frequency (among activated ($CD44^{hi}$) $CD4^+$ T cells) and total number of T_{FH} cells and GC T_{FH} cells in spleens of mice as in **a** ($n = 7$ per group). (**c**) Flow cytometry of total $B220^+$ B cells from mice as in **a**. Numbers adjacent to outlined areas indicate percent $GL7^+Fas^+$ GC B cells (top row) or $CD138^+IgD^{lo}$ plasma cells (bottom row). (**d**) Frequency (among total $B220^+$ B cells) and total number of GC B cells and plasma cells in the spleen of mice as in **a** ($n = 7$ per group). (**e**) ELISA of VACV-specific IgG in serum from infected mice as in **a** or uninfected B6 mice (Naive) ($n = 4$ per group), presented as absorbance at 450 nm (A_{450}). (**f**) Flow cytometry assessing polyclonal T_{FH} cells and GC T_{FH} cells from wild-type and Itch-cKO mice 8 d after infection with VACV (numbers in plots as in **a**). (**g**) Frequency (among activated ($CD44^{hi}$) $CD4^+$ T cells) and total number of T_{FH} cells and GC T_{FH} cells in the spleen of mice as in **f** ($n = 6$ per group). (**h**) Flow cytometry assessing GC B cells and plasma cells from mice as in **f** (numbers in plots as in **c**). (**i**) Frequency (among total $B220^+$ B cells) and total number of GC B cells and plasma cells in the spleen of mice as in **f** ($n = 6$ per group). (**j**) ELISA of VACV-specific IgG in serum from mice as in **f** ($n = 3$ per group). Each symbol (**b**,**d**,**g**,**i**) represents an individual mouse; small horizontal lines indicate the mean (±s.d.). $^*P < 0.01$ and $^{**}P < 0.001$ (Student's *t*-test). Data are representative of at least three independent experiments (error bars, s.d.).

As ICOS is required for Bcl-6 expression at day 3 after infection *in vivo*[14], we quantified *Icos* expression in wild-type and *Itch*$^{-/-}$ SMARTA $CD4^+$ T cells. Although *Itch*$^{-/-}$ SMARTA $CD4^+$ T cells failed to differentiate into T_{FH} cells, their expression of *Icos* mRNA and ICOS protein was similar to that of wild-type SMARTA $CD4^+$ T cells (**Fig. 2c** and **Supplementary Fig. 2c**). Moreover, the expression of genes encoding some transcription factors upstream of Bcl-6, such as *Batf* and *Irf4*, was also intact in *Itch*$^{-/-}$ SMARTA $CD4^+$ T cells (**Fig. 2c**). These results indicated that the defective differentiation of *Itch*$^{-/-}$ T_{FH} cells was not due to changes in the expression of ICOS or known transcription factors upstream of Bcl-6.

We next investigated whether the early defect in *Itch*$^{-/-}$ T_{FH} cells continued through the peak of the LCMV-specific response (day 8) and whether it affected GC T_{FH} cell development. *Itch*$^{-/-}$ SMARTA $CD4^+$ T cells showed normal proliferation at day 8 after infection with LCMV (**Supplementary Fig. 2d**). Notably, we observed an almost complete loss of T_{FH} cells among *Itch*$^{-/-}$ SMARTA $CD4^+$ T cells (**Fig. 2d,e**). There were almost no GC T_{FH} cells ($CXCR5^+PD\text{-}1^{hi}$, $CXCR5^+Bcl\text{-}6^{hi}$ or $CXCR5^+GL7^{hi}$) among *Itch*$^{-/-}$ SMARTA $CD4^+$ T cells (**Fig. 2d,e** and **Supplementary Fig. 2e**). In addition, *Itch*$^{-/-}$ SMARTA $CD4^+$ T cells were unable to upregulate expression of CXCR5 or Bcl-6 at day 8 after infection with LCMV (**Supplementary Fig. 2f**). Collectively, these results demonstrated that Itch was required for the differentiation of T_{FH} cells both at early stages and late stages and that Itch regulated T_{FH} cell differentiation in a cell-intrinsic manner.

Defective differentiation of T_{FH} cells unrelated to T_H2 bias

Itch associates with JunB and c-Jun and promotes their ubiquitination and subsequent degradation. The increased amount of JunB protein in *Itch*$^{-/-}$ T cells drives T_H2-biased differentiation and leads to elevated production of canonical T_H2 cell cytokines, particularly IL-4 (ref. 26). IL-4 is also one of the cytokines produced by T_{FH} cells, especially by GC T_{FH} cells[32,33], and has long been recognized as a factor involved in the survival and differentiation of B cells. However, IL-4 and its signaling pathways are not required for T_{FH} cell differentiation[11,34,35]. *Il4*$^{-/-}$ mice exhibited a frequency and number of total T_{FH} cells and GC T_{FH} cells similar to that of wild-type mice in

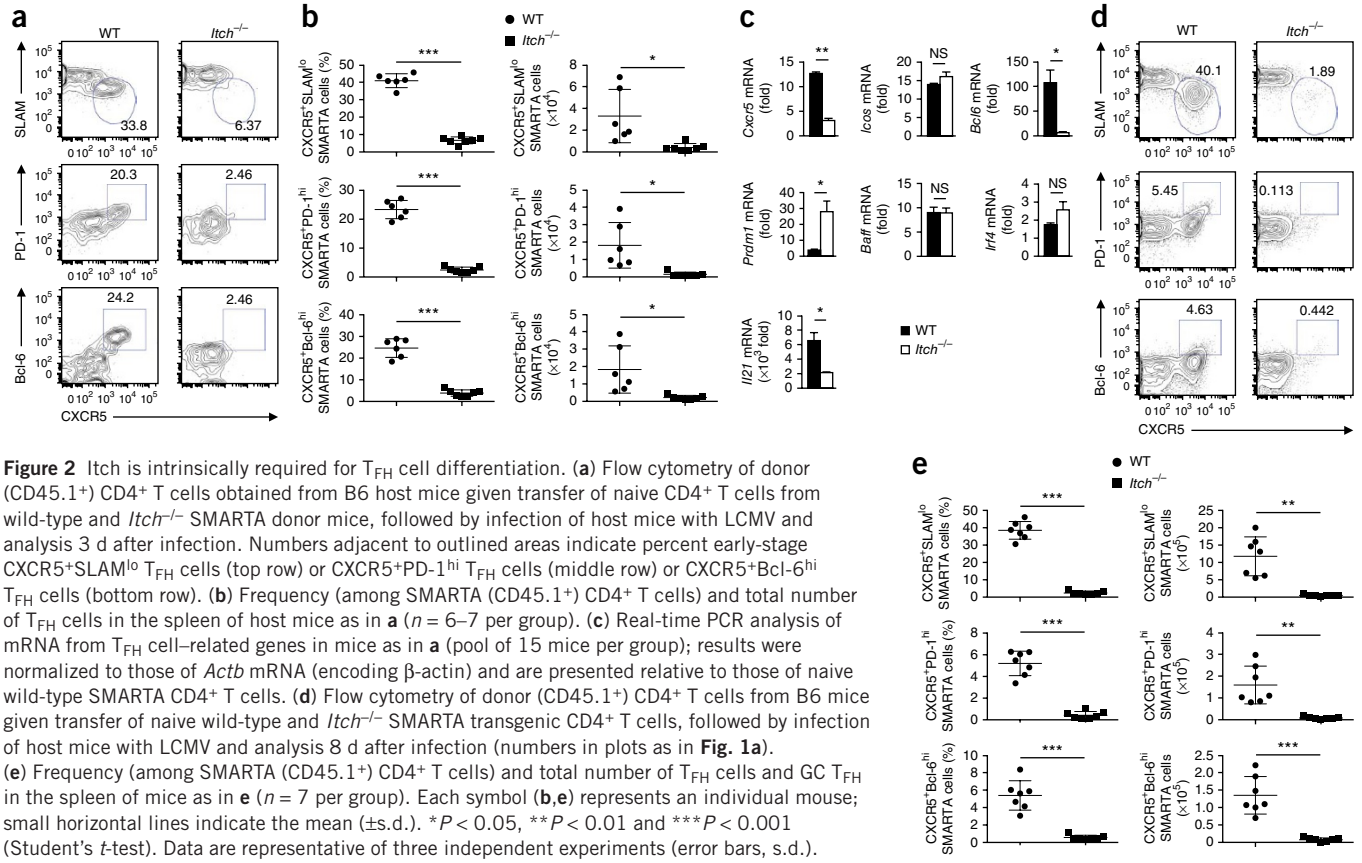

Figure 2 Itch is intrinsically required for T_{FH} cell differentiation. (**a**) Flow cytometry of donor (CD45.1$^+$) CD4$^+$ T cells obtained from B6 host mice given transfer of naive CD4$^+$ T cells from wild-type and *Itch*$^{-/-}$ SMARTA donor mice, followed by infection of host mice with LCMV and analysis 3 d after infection. Numbers adjacent to outlined areas indicate percent early-stage CXCR5$^+$SLAM^{lo} T_{FH} cells (top row) or CXCR5$^+$PD-1^{hi} T_{FH} cells (middle row) or CXCR5$^+$Bcl-6^{hi} T_{FH} cells (bottom row). (**b**) Frequency (among SMARTA (CD45.1$^+$) CD4$^+$ T cells) and total number of T_{FH} cells in the spleen of host mice as in **a** (n = 6–7 per group). (**c**) Real-time PCR analysis of mRNA from T_{FH} cell–related genes in mice as in **a** (pool of 15 mice per group); results were normalized to those of *Actb* mRNA (encoding β-actin) and are presented relative to those of naive wild-type SMARTA CD4$^+$ T cells. (**d**) Flow cytometry of donor (CD45.1$^+$) CD4$^+$ T cells from B6 mice given transfer of naive wild-type and *Itch*$^{-/-}$ SMARTA transgenic CD4$^+$ T cells, followed by infection of host mice with LCMV and analysis 8 d after infection (numbers in plots as in **Fig. 1a**). (**e**) Frequency (among SMARTA (CD45.1$^+$) CD4$^+$ T cells) and total number of T_{FH} cells and GC T_{FH} in the spleen of mice as in **e** (n = 7 per group). Each symbol (**b**,**e**) represents an individual mouse; small horizontal lines indicate the mean (±s.d.). $*P < 0.05$, $**P < 0.01$ and $***P < 0.001$ (Student's t-test). Data are representative of three independent experiments (error bars, s.d.).

response to acute infection with VACV (**Fig. 3a**,**b**). Nevertheless, we next investigated further to confirm that the defect in T_{FH} cell differentiation in *Itch*$^{-/-}$ mice was not due to T_H2-biased differentiation or chronic inflammation caused by overproduction of IL-4. To address this, we crossed *Itch*$^{-/-}$ mice or Itch-cKO mice with *Il4*$^{-/-}$ mice to generate mice deficient in both Itch and IL-4 (Itch–IL-4–DKO mice). We infected the progeny with VACV and analyzed their T cell and B cell responses. We first assessed the differentiation of T_{FH} cells in Itch–IL-4–DKO mice. The differentiation of T_{FH} cells and GC T_{FH} cells was considerably impaired in Itch–IL-4–DKO mice compared with that in wild-type mice (**Fig. 3c**,**d**). The differentiation of T_{FH} and GC T_{FH} cells in Itch–IL-4–DKO was not greater than that in *Itch*$^{-/-}$ mice (**Fig. 3c**,**d**). Consistent with the reduced number of GC B cells and plasma cells in *Itch*$^{-/-}$ mice, the number of GC B cells and plasma cells in Itch–IL-4–DKO mice was also much lower than that of wild-type mice (**Fig. 3e**,**f** and **Supplementary Fig. 3a**). Furthermore, the GC B cell and plasma cell responses of Itch–IL-4–DKO mice were not enhanced relative to those of *Itch*$^{-/-}$ mice (**Fig. 3e**,**f** and **Supplementary Fig. 3a**), which suggested that the defect in the development of GC B cells and plasma cells in *Itch*$^{-/-}$ mice could not be 'rescued' by deletion of IL-4. Collectively, these data suggested that IL-4 did not affect T_{FH} cell differentiation and that the defect in T_{FH} cell differentiation in *Itch*$^{-/-}$ mice was independent of T_H2 cells.

As an additional investigation of T_H2 signaling, we next assessed whether the defective differentiation of T_{FH} cells of *Itch*$^{-/-}$ mice could be rectified by JunB deficiency. For this, we knocked down JunB in *Itch*$^{-/-}$ and *Itch*$^{+/+}$ (wild-type) SMARTA bone marrow through the use of short hairpin RNA (shRNA) and generated chimeras reconstituted with that bone marrow. We isolated naive SMARTA CD4$^+$ T cells from the reconstituted mice and then adoptively transferred these cells into B6 recipient mice, followed by infection of the hosts with LCMV. Deficiency of JunB did not restore the T_{FH}-differentiation defect of *Itch*$^{-/-}$ T cells (**Supplementary Fig. 3b**,**c**). These data further confirmed that the defect in T_{FH} cell differentiation in *Itch*$^{-/-}$ mice was independent of T_H2 cells.

IL-2 signaling is not responsible for the T_{FH} cell defect

It has been reported that IL-2 inhibits differentiation into T_{FH} cells[16,17] and is in fact dose-limiting for differentiation into T_H1 cells versus T_{FH} cells in response to an acute infection with LCMV, as twofold lower expression of the receptor for IL-2 (IL-2R) is sufficient to double the frequency of T_{FH} cells[19]. At day 3 after infection of wild-type and *Itch*$^{-/-}$ SMARTA mice with LCMV, expression of the α-chain of IL-2R (IL-2Rα) in SMARTA *Itch*$^{-/-}$ non-T_{FH} (T_H1) CD4$^+$ T cells was similar to that in their wild-type counterparts (**Supplementary Fig. 3e**). However, additional results suggested that Itch might target IL-2Rγ for ubiquitination (data not shown). We explored the possibility that the T_{FH}-differentiation defect of *Itch*$^{-/-}$ CD4 T cells was due to enhanced IL-2 signaling. We transferred wild-type SMARTA CD4$^+$ T cells or *Itch*$^{-/-}$ SMARTA CD4$^+$ T cells into B6 mice that we subsequently infected with LCMV. We treated the recipient mice with neutralizing antibody to IL-2 (anti-IL-2) or isotype-matched control antibody 1 d before and 1 d after infection. Consistent with a published report[16], neutralization of IL-2 significantly enhanced the commitment of wild-type SMARTA cells to T_{FH} differentiation at day 3 after infection, from 17% to 36% (**Fig. 4**). However, neither the frequency of T_{FH} cells (CXCR5$^+$SLAM^{lo} cells or CXCR5$^+$Bcl-6^{hi}) nor the expression of CXCR5 and Bcl-6 protein was restored in *Itch*$^{-/-}$ CD4 T cells by neutralization of IL-2 (**Fig. 4**). We also knocked down IL-2Rγ in primary SMARTA CD4$^+$ T cells through the use of shRNA

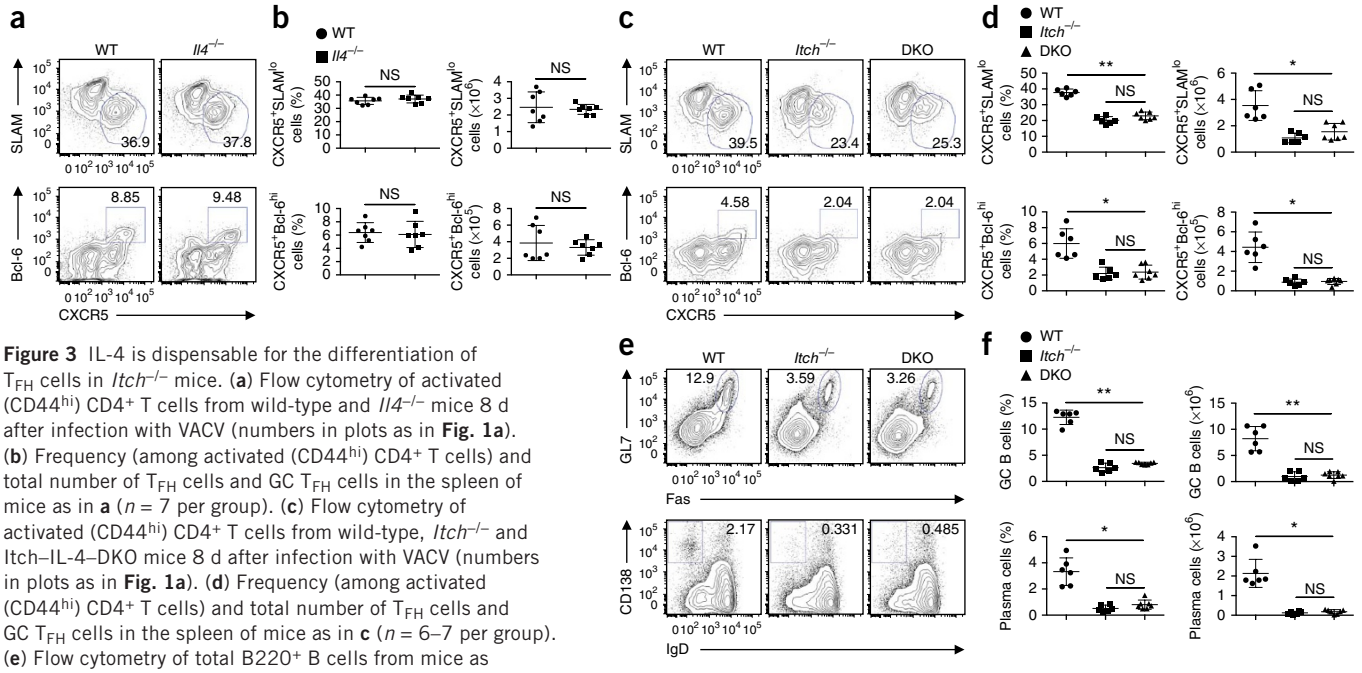

Figure 3 IL-4 is dispensable for the differentiation of T_{FH} cells in *Itch*$^{-/-}$ mice. (**a**) Flow cytometry of activated (CD44^{hi}) CD4$^+$ T cells from wild-type and *Il4*$^{-/-}$ mice 8 d after infection with VACV (numbers in plots as in **Fig. 1a**). (**b**) Frequency (among activated (CD44^{hi}) CD4$^+$ T cells) and total number of T_{FH} cells and GC T_{FH} cells in the spleen of mice as in **a** ($n = 7$ per group). (**c**) Flow cytometry of activated (CD44^{hi}) CD4$^+$ T cells from wild-type, *Itch*$^{-/-}$ and Itch–IL-4–DKO mice 8 d after infection with VACV (numbers in plots as in **Fig. 1a**). (**d**) Frequency (among activated (CD44^{hi}) CD4$^+$ T cells) and total number of T_{FH} cells and GC T_{FH} cells in the spleen of mice as in **c** ($n = 6$–7 per group). (**e**) Flow cytometry of total B220$^+$ B cells from mice as in **c** (numbers in plots as in **Fig. 1c**). (**f**) Frequency (among total B220$^+$ B cells) and total number of GC B cells and plasma cells from mice as in **c** ($n = 6$–7 per group). Each symbol (**b**,**d**,**f**) represents an individual mouse; small horizontal lines indicate the mean (±s.d.). NS, not significant; $^*P < 0.01$ and $^{**}P < 0.001$ (Student's *t*-test). Data are representative of three independent experiments.

and examined T_{FH} cell differentiation *in vivo*. Knockdown of IL-2Rγ increased the frequency of wild-type SMARTA T_{FH} cell but did not rectify the T_{FH}-differentiation defect of *Itch*$^{-/-}$ SMARTA CD4$^+$ T cells (**Supplementary Fig. 3d,e**). Collectively, our data indicated that IL-2 signaling was probably not the key factor that led to the impaired T_{FH} differentiation of *Itch*$^{-/-}$ cells.

'Rescue' by enforced expression of Bcl-6

As Bcl-6 has been identified as the critical transcription factor in the differentiation of T_{FH} cells and its expression was substantially reduced in *Itch*$^{-/-}$ CD4$^+$ T cells, we explored whether Bcl-6 is a potential target of Itch. We found that Itch associated with Bcl-6 both *in vivo* by coimmunoprecipitation and *in vitro* by precipitation assay, and we further identified a Pro-Pro-X-Tyr motif (where 'X' is any amino acid) at positions 182–185 in Bcl-6 that was responsible for the interaction (**Supplementary Fig. 4a**,**b**). In addition, Itch promoted both monoubiquitination and polyubiquitination of Bcl-6 (**Supplementary Fig. 4c**). To investigate the physiological function of the modification of Bcl-6 by Itch, we transduced wild-type SMARTA CD4$^+$ T cells with a retroviral vector expressing green fluorescent protein (GFP) alone (empty vector) or GFP and either wild-type Bcl-6 or mutant Bl-6 with replacement of phenylalanine with tyrosine, then sorted the transduced cells and transferred them into B6 recipient mice, followed by infection of the host mice with LCMV. Expression of the mutant Bcl-6 induced differentiation into T_{FH} cells and GC T_{FH} cells similar to that induced by wild-type Bcl-6 (**Supplementary Fig. 4d**,**e**). These results suggested that modification of Bcl-6 by Itch might not have an apparent physiological function in T_{FH} cell differentiation.

We then investigated whether enforced expression of Bcl-6 was able to rectify the defective T_{FH} differentiation of *Itch*$^{-/-}$ CD4$^+$ T cells. We transduced wild-type or *Itch*$^{-/-}$ SMARTA CD4$^+$ T cells with retroviral vector expressing Bcl-6 or empty vector (as described above). Bcl-6 expression drove more robust T_{FH} differentiation of wild-type SMARTA CD4$^+$ T cells *in vivo* (80%) than did expression of GFP only by the empty vector (37%)[4] (**Fig. 5**). Notably, Bcl-6 expression also substantially enhanced the T_{FH} differentiation of *Itch*$^{-/-}$ SMARTA CD4$^+$ T cells (70% versus 6%), nearly to the extent of that of wild-type SMARTA CD4$^+$ T cells (70% versus 80%; **Fig. 5**). Furthermore, Bcl-6 expression induced similar CXCR5 expression in wild-type and *Itch*$^{-/-}$ SMARTA CD4$^+$ T cells (**Fig. 5b**). These results indicated that Itch might function mainly upstream of Bcl-6 expression and might be required for the induction of Bcl-6 expression and T_{FH} cell differentiation.

Foxo1 as a target for Itch

We next looked for other potential targets of Itch that may be involved in regulating the differentiation of T_{FH} cells, with a particular interest in upstream regulators of Bcl-6. Foxo proteins belong to the forkhead-box family of transcription factors, which are characterized by a conserved winged-helix DNA-binding domain called the 'forkhead' domain. Foxo transcription factors are subject to extensive and varied post-translational modifications that affect their abundance, localization and transcriptional activity, with ubiquitination being one major pathway by which Foxo factors are regulated[36]. It has been well documented that the Foxo family can be negatively regulated by the signaling pathways of phosphatidylinositol-3-OH kinase (PI(3)K) and the kinase Akt in response to insulin, growth factors or the engagement of costimulatory receptors (CD28 and ICOS)[36,37]. Phosphorylation of Foxo factors at three conserved sites (Tyr24, Ser256 and Ser319) by the kinases Akt and SGK ('serum and glucocorticoid-induced kinase') causes their export from the nucleus and degradation and thereby prevents Foxo factors from transactivating or repressing their target genes[36]. Ubiquitination and degradation of Foxo1 can be mediated by SKP1–CUL1–F-box protein–SKP2 complex[38]. Relevant to our study here, Foxo1 has been linked to the regulation of T_{FH} cells either in a positive manner or a negative manner[18,39]. However, the importance of the involvement of Foxo1 or its homologs in the differentiation of T_{FH} cells remains

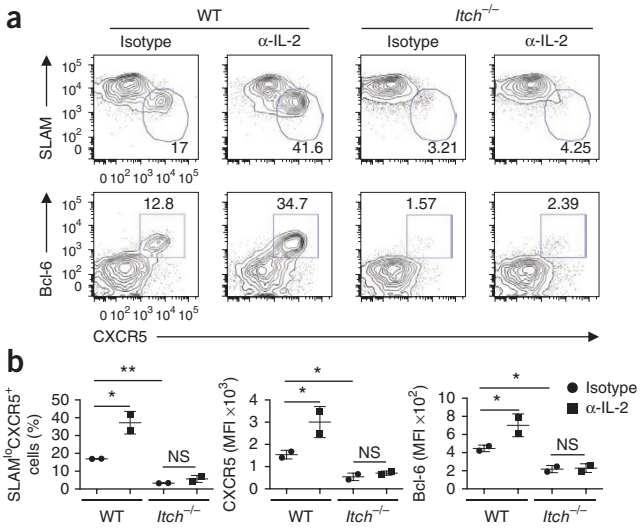

Figure 4 Blockade of IL-2 signaling does not restore the T_{FH} differentiation of *Itch*$^{-/-}$ cells. (**a**) Flow cytometry of donor (CD45.1$^+$) CD4$^+$ T cells obtained from B6 host mice given adoptive transfer of naive wild-type or *Itch*$^{-/-}$ SMARTA CD4$^+$ T cells, followed by infection of the recipient mice with LCMV 1 d later, along with treatment of the recipient mice with neutralizing antibody to IL-2 (α-IL-2) or isotype-matched control antibody (Isotype) 1 d before and 1 d after infection, and analysis of splenocytes 3 d after infection. Numbers adjacent to outlined areas indicate percent SLAM^{lo}CXCR5$^+$ cells (top) or Bcl-6^{hi}CXCR5$^+$ cells (bottom), identified as early-stage T_{FH} cells. (**b**) Quantification of SLAM^{lo}CXCR5$^+$ T_{FH} cells among total SMARTA CD4$^+$ T cells (left), and expression of CXCR5 (middle) and Bcl-6 (right), presented as mean fluorescence intensity (MFI), for cells from host mice in **a**. Each symbol represents an individual mouse; small horizontal lines indicate the mean (±s.d.). $^*P < 0.05$ and $^{**}P < 0.001$ (Student's *t*-test). Data are representative of two independent experiments two mice per group.

unclear, and the underlying molecular mechanisms by which Foxo1 is regulated in this process have not been elucidated so far.

We then investigated whether Foxo1 is a substrate of Itch. Given the presence of proline-rich sequences in Foxo proteins, we assessed the ability of Itch to recognize Foxo proteins. We first coimmunoprecipitated proteins from Jurkat human T lymphocyte cells that overexpressed Foxo proteins and Itch. Only Foxo1 immunoprecipitated together with Itch, whereas Foxo3a protein did not (**Fig. 6a**), which suggested that Itch selectively interacted with Foxo1. Notably, we also detected endogenous interaction between Foxo1 and Itch in purified CD4$^+$ T cells from VACV-infected B6 mice (**Fig. 6b**), which suggested that this interaction was physiologically functional. More notably, the interaction between Foxo1 and Itch in CD4$^+$ T cell blasts was rapidly induced by restimulation with monoclonal anti-ICOS and monoclonal anti-CD3 (**Fig. 6c**).

To investigate whether Itch promoted the ubiquitination of Foxo1, we transfected Jurkat T cells with plasmids expressing hemagglutinin-tagged ubiquitin and Myc-tagged Foxo1 (and Xpress-tagged wild-type Itch). We then either left the cells untreated or treated them with the proteasome inhibitor MG132 and then immunoprecipitated proteins from cell lysates with anti-Foxo1. Overexpression of wild-type Itch enhanced the conjugation of ubiquitin to Foxo1 in the presence of MG132 (**Fig. 6d**). To assess the *in vivo* ubiquitination of Foxo1, we generated a new rabbit polyclonal antibody to ubiquitin and used this antibody in an assay in which we immunoprecipitated ubiquitinated protein. In these experiments, we pretreated CD4$^+$ T cell blasts with MG132 and then restimulated them with monoclonal anti-CD3 and monoclonal anti-ICOS. After restimulation, we immunoprecipitated proteins from lysates of *Itch*$^{-/-}$ or wild-type CD4$^+$ T cells with the polyclonal antibody to ubiquitin. We detected polyubiquitinated Foxo1 as slowly migrating, high-molecular-weight species in wild-type cells that was almost completely absent from *Itch*$^{-/-}$ cells (**Fig. 6e**). Together these results suggested that Itch acted as an E3 ligase for the ubiquitination of Foxo1.

It has been reported that the PI(3)K-Akt pathway induces the phosphorylation of Foxo1 and promotes its degradation and that ICOS regulates T_{FH} cell differentiation through the PI(3)K-Akt pathway[37,40]. These reports prompted us to investigate whether an ICOS-PI(3)K-Akt pathway induces the degradation of Foxo1 by Itch. We examined the signal-transduction events and their consequences in ICOS-stimulated wild-type and Itch-deficient T cells. As described above, we restimulated CD4$^+$ T cell blasts with monoclonal anti-CD3 and monoclonal anti-ICOS. Consistent with published findings[40], engagement of ICOS substantially enhanced the activation of Akt mediated via the T cell antigen receptor, as indicated by increased phosphorylation of Akt at Ser473 in wild-type CD4$^+$ T cells (**Fig. 6f**). Phosphorylation of Foxo1 was also enhanced by ligation of ICOS in wild-type CD4$^+$ T cells. However, phosphorylation of Akt Ser473 and Foxo1 was similarly increased by ligation of ICOS in Itch-deficient CD4$^+$ T cells. Notably, engagement of ICOS resulted in decreased expression of Foxo1 protein after 10 min of stimulation in wild-type CD4$^+$ T cells. In contrast, the expression of Foxo1 protein remained largely unchanged in Itch-deficient T cells. Together these results suggested that Itch was not involved in the ICOS-triggered signaling events that resulted in the phosphorylation of Foxo1 but that Itch was critically required for the degradation of Foxo1 protein.

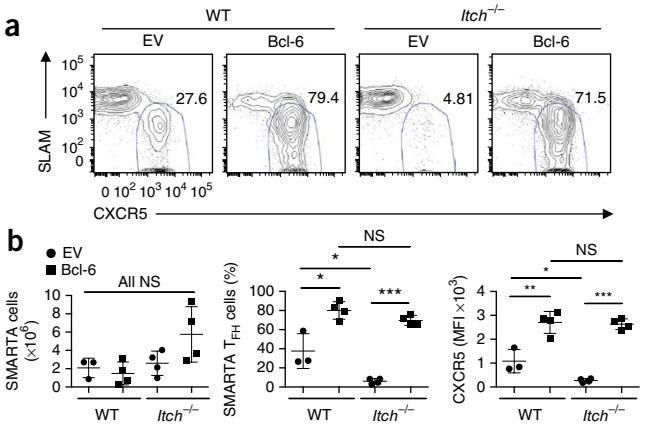

Figure 5 Restoration of the defective T_{FH} differentiation of *Itch*$^{-/-}$ cells by overexpression of Bcl-6. (**a**) Flow cytometry of donor (CD45.1$^+$) CD4$^+$ T cells obtained from B6 host mice given adoptive transfer of wild-type or *Itch*$^{-/-}$ SMARTA CD4$^+$ T cells transduced with retroviral vector expressing GFP only (empty vector (EV)) or GFP and Bcl-6 (Bcl-6), followed by infection of recipient mice with LCMV and analysis 8 d after infection. Numbers adjacent to outlined areas indicate percent SLAM^{lo}CXCR5$^+$ cells (T_{FH} cells). (**b**) Proliferation of SMARTA CD4$^+$ T cells, quantified as total SMARTA cells in the spleen (left), frequency of T_{FH} cells among SMARTA (CD45.1$^+$) CD4$^+$ T cells (middle), and CXCR5 expression, presented as mean fluorescence intensity (right), for cells from host mice in **a**. Each symbol represents an individual mouse; small horizontal lines indicate the mean (±s.d.). $^*P < 0.05$, $^{**}P < 0.01$ and $^{***}P < 0.001$ (Student's *t*-test). Data are representative of three independent experiments with three to four mice per group.

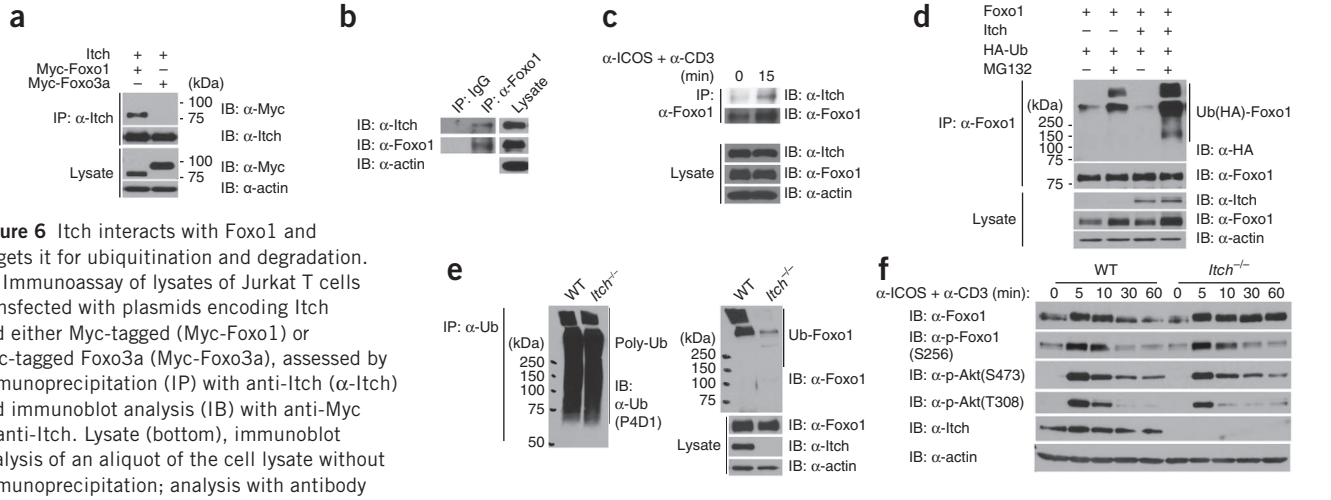

Figure 6 Itch interacts with Foxo1 and targets it for ubiquitination and degradation. (**a**) Immunoassay of lysates of Jurkat T cells transfected with plasmids encoding Itch and either Myc-tagged (Myc-Foxo1) or Myc-tagged Foxo3a (Myc-Foxo3a), assessed by immunoprecipitation (IP) with anti-Itch (α-Itch) and immunoblot analysis (IB) with anti-Myc or anti-Itch. Lysate (bottom), immunoblot analysis of an aliquot of the cell lysate without immunoprecipitation; analysis with antibody to β-actin (α-actin) serves as a loading control (throughout). Right margin, molecular size in kilodaltons (kDa). (**b**) Immunoassay of combined cytosolic and nuclear fractions of $CD4^+$ T cells purified from B6 mice 8 d after infection with VACV, assessed by immunoprecipitation with IgG (isotype-matched control antibody) or anti-Foxo1 and immunoblot analysis with anti-Itch or anti-Foxo1. (**c**) Immunoassay of combined cytosolic and nuclear fractions of $CD4^+$ T cell blasts stimulated for 0 or 15 min with anti-CD3 (3 μg/ml) and anti-ICOS (2 μg/ml), assessed by immunoprecipitation with anti-Foxo1 and immunoblot analysis with anti-Itch or anti-Foxo1. (**d**) Immunoassay of Jurkat T cells transfected with plasmids encoding Foxo1 and wild-type Itch and/or hemagglutinin-tagged ubiquitin (HA-Ub), then left untreated (–) or treated (+) for 1 h with MG132 (25 μM), assessed by denaturation of lysates in 1% SDS, immunoprecipitation with anti-Foxo1 and immunoblot analysis with anti-hemagglutinin (anti-HA) and anti-Foxo1 (lysates without immunoprecipitation probed with anti-Itch or anti-Foxo1). Ub(HA)-Foxo1 (top right), hemagglutinin-tagged ubiquitinated Foxo1. (**e**) Immunoassay of wild-type or *Itch*$^{-/-}$ $CD4^+$ T cell blasts pretreated with MG132 and stimulated for 20 min with anti-CD3 (3 μg/ml) and anti-ICOS (2 μg/ml), assessed by denaturation of lysates in 1% SDS, immunoprecipitation with polyclonal anti-ubiquitin (α-Ub) and immunoblot analysis with monoclonal anti-ubiquitin (P4D1; left blot) or anti-Foxo1 (top right blot); lysates without immunoprecipitation (bottom right blot) probed with anti-Foxo1, anti-Itch or anti-β-actin. Poly-Ub, polyubiquitination; Ub-Foxo1, ubiquitinated Foxo1. (**f**) Immunoblot analysis of lysates of wild-type or *Itch*$^{-/-}$ $CD4^+$ T cell blasts stimulated for 0–60 min (above lanes) with anti-CD3 (3 μg/ml) and anti-ICOS (2 μg/ml), probed with anti-Foxo1 (α-Foxo1), antibody to Foxo1 phosphorylated at Ser256 (α-p-Foxo1(S256)), antibody to Akt phosphorylated at Ser473 (α-p-Akt(S473)) or Thr308 (α-p-Akt(T308)), anti-Itch (α-Itch) or anti-β-actin (α-actin). Data are representative of two independent experiments.

Foxo1 ablation rectifies defective T_{FH} cell differentiation

The expression of Foxo1 protein was much lower in T_{FH} cells than in naive cells or non-T_{FH} cells and was even lower in GC T_{FH} cells (**Fig. 7a**). Notably, the expression of *Foxo1* mRNA was substantial in each population (**Fig. 7a**), consistent with a central role for post-translational degradation in the control of Foxo1 expression. However, the expression of Itch protein and *Itch* mRNA was retained in all populations (**Fig. 7a**). This indicated that T_{FH} cell differentiation might require downregulation of Foxo1 expression through post-translational modification by Itch. We therefore tested mice conditionally deficient in Foxo1 or Foxo3a. The differentiation of T_{FH} cells in response to acute infection with VACV was enhanced in *Foxo1*$^{fl/fl}$CD4-Cre mice compared with that of their wild-type (*Foxo1*$^{+/+}$ CD4-Cre or *Foxo1*$^{fl/fl}$) counterparts (**Supplementary Fig. 5a**). Consequently, the number of GC B cells and plasma cells was also greater in *Foxo1*$^{fl/fl}$CD4-Cre mice than in their wild-type counterparts after infection with VACV (**Supplementary Fig. 5b**). However, *Foxo3a*$^{fl/fl}$CD4-Cre mice showed normal differentiation of T_{FH} cells, as well as normal development of GC B cells and plasma cells after infection (**Supplementary Fig. 5c,d**). These results suggested that Foxo1 was a negative regulator of the differentiation of T_{FH} cells.

We next sought to determine whether Itch affects Foxo1-mediated gene expression. We sorted wild-type and *Itch*$^{-/-}$ SMARTA $CD4^+$ T cells from B6 recipient mice at day 3 after infection with LCMV and analyzed expression of Foxo1 targets by real-time PCR. *Itch*$^{-/-}$ cells had much higher expression of several known Foxo1 targets[41,42], such as *Bcl2l11, Il7r, Klf2, Sell, Selplg* and *S1pr1*, than did wild-type SMARTA $CD4^+$ T cells (**Fig. 7b**). These data suggested that Itch suppressed the expression of at least some of Foxo1 targets.

We then investigated whether the defective differentiation of T_{FH} cells in *Itch*$^{-/-}$ mice could be restored by genetic ablation of Foxo1. Because of the technical difficulty in generating *Itch*$^{fl/fl}$*Foxo1*$^{fl/fl}$ CD4-Cre^+ mice, we crossed *Itch*$^{fl/fl}$*Foxo1*$^{fl/fl}$ mice with transgenic mice in which Cre recombinase is under control of the interferon-responsive *Mx1* promoter to generate *Itch*$^{fl/fl}$*Foxo1*$^{fl/fl}$Mx1-Cre mice with inducible deficiency in both Itch and Foxo1 (Itch-Foxo1-iDKO mice). Immunoblot analysis revealed that the expression of Itch and/or Foxo1 was almost completely eliminated in splenocytes 2 weeks after injection of the synthetic RNA duplex poly (I:C) (polyinosine-polycytidylic acid) (**Supplementary Fig. 6a**). Following infection with VACV, the development of GC B cells in *Itch*$^{fl/fl}$Mx1-Cre mice with inducible deficiency in Itch (Itch-iKO) was much lower than that in their wild-type counterparts (**Fig. 7c,d** and **Supplementary Fig. 6b,c**), consistent with the phenotype of *Itch*$^{-/-}$ mice and Itch-cKO mice. Likewise, the development of plasma cells was also significantly lower in Itch-iKO mice than in their wild-type counterparts (**Fig. 7c,d** and **Supplementary Fig. 6b,c**). Unexpectedly, the development of both GC B cells and plasma cells in Itch-Foxo1-iDKO mice was increased to their development in wild-type mice (**Fig. 7c,d** and **Supplementary Fig. 6b,c**). We next examined the differentiation of T_{FH} cells and GC T_{FH} cells. The frequency and absolute number of T_{FH} cells was much lower in Itch-iKO mice than in wild-type mice (**Fig. 7e,f** and **Supplementary Fig. 6c**). The frequency and number of GC T_{FH} cells was also lower in Itch-iKO mice than in wild-type mice. Notably, the differentiation of T_{FH} cells and GC T_{FH} cells was restored in Itch-Foxo1-iDKO mice (**Fig. 7e,f** and **Supplementary Fig. 6c**). In contrast, IL-4 production in $CD4^+$ T cells from Itch-iKO mice was similar to that in $CD4^+$ T cells from Itch-Foxo1-iDKO mice

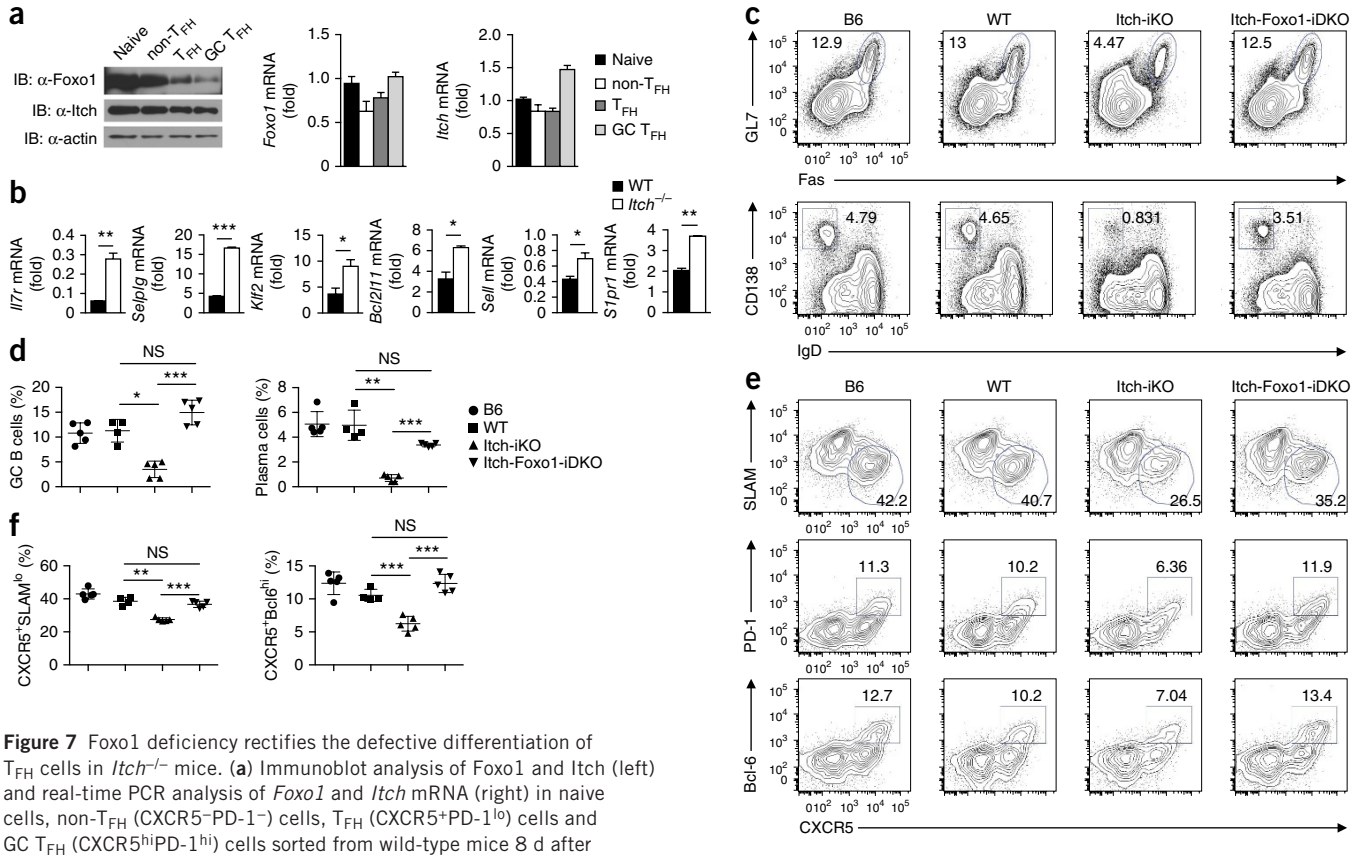

Figure 7 Foxo1 deficiency rectifies the defective differentiation of T_{FH} cells in *Itch*$^{-/-}$ mice. (**a**) Immunoblot analysis of Foxo1 and Itch (left) and real-time PCR analysis of *Foxo1* and *Itch* mRNA (right) in naive cells, non-T_{FH} (CXCR5^{-}PD-1^{-}) cells, T_{FH} (CXCR5^{+}PD-1^{lo}) cells and GC T_{FH} (CXCR5^{hi}PD-1^{hi}) cells sorted from wild-type mice 8 d after infection with VACV; mRNA results were normalized to those of *Actb* mRNA and are presented relative to those of naive cells, set as 1. (**b**) Real-time PCR analysis of the mRNA products of Foxo1 targets in donor CD4^{+} T cells from B6 recipient mice given transfer of CD4^{+} T cells from wild-type or *Itch*$^{-/-}$ SMARTA donor mice, followed by infection of recipients with LCMV and analysis 3 d later; mRNA results were normalized to those of *Actb* mRNA and are presented relative to those of naive wild-type SMARTA CD4^{+} T cells, set as 1. (**c**) Flow cytometry of splenocytes from B6 mice not treated with poly(I:C) (far left) or from wild-type (*Itch*$^{fl/fl}$) mice (WT), Itch-iKO mice and Itch-Foxo1-iDKO mice given intraperitoneal injection of poly(I:C), followed by infection of all mice with VACV 2 weeks later and analysis 8 d after infection (numbers in plots as in **Fig. 1c**). (**d**) Frequency of GC B cells and plasma cells among B220^{+} B cells from mice as in **c** (n = 4–5 per group). Each symbol represents an individual mouse; small horizontal lines indicate the mean (±s.d.). (**e**) Flow cytometry of activated (CD44^{hi}) CD4^{+} T cells from mice as in **c** (numbers in plots as in **Fig. 1a**). (**f**) Frequency of T_{FH} cells and GC (CXCR5^{+}Bcl-6^{hi}) T_{FH} cells among activated (CD44^{hi}) CD4^{+} T cells from mice as in **c** (n = 4–5 per group). *P < 0.05, **P < 0.01 and ***P < 0.001 (Student's t-test). Data are representative of two experiments (**a**,**b**; error bars, s.d.) or at least three experiments (**c**–**f**).

(**Supplementary Fig. 6d**). These results indicated that deletion of Foxo1 did not affect Itch-mediated production of IL-4. Together these data suggested that the defect in the differentiation of GC B cells and T_{FH} cells in *Itch*$^{-/-}$ mice could be 'rescued' by genetic ablation of Foxo1.

To investigate whether the restoration of T_{FH} cell differentiation in *Itch*$^{-/-}$ mice via deficiency in Foxo1 was cell intrinsic, we knocked down Foxo1 expression in wild-type or *Itch*$^{-/-}$ SMARTA CD4^{+} T cells with a retrovirus encoding shRNA and transferred transduced and untransduced cells together into B6 recipient mice, followed by infection of the host mice with LCMV. Transduction of control shRNA (targeting CD8α) did not alter the T_{FH} differentiation of either wild-type cells or *Itch*$^{-/-}$ cells (**Supplementary Fig. 7a–c**). In contrast, transduction of shRNA targeting Foxo1 substantially enhanced the T_{FH} differentiation of wild-type cells (**Supplementary Fig. 7a–c**). Notably, knockdown of Foxo1at least partially restored the T_{FH} differentiation of *Itch*$^{-/-}$ cells (**Supplementary Fig. 7a–c**). The data further confirmed a critical role for Foxo1 in the regulation of T_{FH} cell differentiation by Itch.

DISCUSSION

Accumulating evidence has established T_{FH} cells as a distinct and important type of CD4^{+} helper T cell that has a crucial role in humoral responses to pathogen infection and damaging roles in autoimmune diseases. Bcl-6 has been identified as a master regulator of T_{FH} cell differentiation[4–6]. However, how Bcl-6 is induced and how T_{FH} cell differentiation is regulated still has many unknown aspects[19]. In this study, through the use of a combination of genetic, cellular and molecular approaches, we have identified a previously unknown and critical function for Itch in T_{FH} cell differentiation and humoral immunity. We have shown that Itch was intrinsically required for both early stages and late stages of T_{FH} cell differentiation and was associated with a substantial reduction in Bcl-6 expression. Finally, we have also shown that Itch regulated T_{FH} cell differentiation by targeting Foxo1, a negative regulator of such differentiation, for degradation.

On the B6 background, *Itch*$^{-/-}$ mice develop chronic inflammatory diseases and constant itching of the skin[43]. Itch inhibits T_H2 differentiation by targeting JunB for ubiquitination and degradation[26]. This might all contribute to the chronic inflammatory diseases of *Itch*$^{-/-}$ mice. However, *Itch*$^{-/-}$ mice unexpectedly showed a substantial defect in T_{FH} cell differentiation in response to viral infection. Although IL-4 is one of the cytokines produced by GC T_{FH} cells that is required for the optimal provision of help to B cells, it has been shown that IL-4 is dispensable for T_{FH} cell differentiation. Our data support that notion and clarify that the defective differentiation of T_{FH} cells in *Itch*$^{-/-}$

mice was not due to T_H2 bias, because T_{FH} cell differentiation was also unaffected in *Il4*$^{-/-}$ mice; the defect in the differentiation of T_{FH} cells in *Itch*$^{-/-}$ mice was not rectified by IL-4 deficiency; and genetic ablation of Foxo1 did rectify the defect in T_{FH} cells in Itch-deficient mice without affecting IL-4 production.

Foxo1 can be targeted for ubiquitination by several ubiquitin E3 ligases, including the SKP1–CUL1–F-box protein–SKP2 complex, MDM2, COP1 and CHIP ('C terminus of Hsc70-interacting protein'), in various cell types[44]. In this study, we identified Itch as an additional E3 ligase that targeted Foxo1 for ubiquitination and degradation. We also established that the ICOS-PI(3)K-Akt pathway led to the ubiquitination and degradation of Foxo1 by Itch. However, future studies are needed to explore details of the mechanism, including the sites modified and the polyubiquitination chain of Foxo1. In addition, the partial 'rescue' of T_{FH} cell differentiation in the experiment in which Foxo1 was knocked down by shRNA might suggest that Itch targets other substrates. Although we found that Bcl-6 itself might be a target, the Itch–Bcl-6 association was not required for the development of T_{FH} cells. The data reinforce the notion that Foxo1 is a critical substrate of multiple Itch targets for T_{FH} cell differentiation. Future efforts should provide a more comprehensive understanding of the molecular interactions among the potential participants.

Emerging evidence has shown that Foxo1 and Foxo3a are involved in immunological regulation. Foxo1 and Foxo3a function redundantly as transcription factors important in the promotion of *Foxp3* expression[27,39,45]. Although Foxo3a can bind and activate the *Bcl6* promoter in B cell lymphoma lines[46], mice with T cell–specific deficiency in Foxo3a exhibited normal T_{FH} cell differentiation. Published studies and also our study here have shown that large numbers of T_{FH} cells accumulate in mice with T cell–specific deficiency in Foxo1 maintained under standard housing conditions[39] or infected with a specific pathogen. However, whether this excessive formation of T_{FH} cells is cell intrinsic or is due to loss of regulatory T cells has remained unclear[39]. A scan of the *Bcl6* promoter identified Foxo-binding motifs in the DNA[18]. Although chromatin-immunoprecipitation experiments have suggested that Foxo1 binds directly to putative Foxo-binding motifs in the *Bcl6* promoter[18,42], the consequence of such binding remains controversial. Luciferase experiments have suggested that Foxo proteins, including Foxo1, activate the *Bcl6* promoter[18]. However, the *in vivo* data we have presented here indicated a negative role for Foxo1 in Bcl-6 expression and T_{FH} cell differentiation. Future studies are needed to clarify this issue. In addition to *Bcl6*, other T_{FH} cell–related genes, such as *Cxcr4, Batf, Icos* and *Prdm1*, have also been reported as containing Foxo1-binding sites identified by chromatin immunoprecipitation followed by deep sequencing[42]. Therefore, Foxo1 may regulate T_{FH} cell differentiation by directly controlling the expression of T_{FH} cell–related genes. Foxo1 can also regulate lymphocyte trafficking by inducing L-selectin and the chemokine receptor CCR7 (ref. 41). The proposal that Foxo1 directly binds to the promoter, untranslated region, introns or intergenic regions of some genes encoding homing molecules, such as *Ccr7, S1pr1, Sell* and *Selplg*, has been further supported by chromatin immunoprecipitation followed by deep sequencing[42]. Two other studies have reported that microRNAs of the miR17~92 family regulate T_{FH} cell differentiation by targeting the PI(3)K antagonist PTEN[47,48] and the phosphatase PHLPP2 (ref. 48) in the ICOS-PI(3)K-Akt pathway. One of those studies also showed that the miR17~92 microRNAs are required for the ability of T_{FH} cells to migrate to B cell follicles and GCs, although no direct mechanism was shown in that study[48]. It is reasonable to speculate that Foxo1 and Itch also regulate T_{FH} cell differentiation at least partially through T cell migration.

In summary, our findings have established a function for Itch as a crucial regulatory factor in T_{FH} cell differentiation. In addition, we have shown that Itch positively regulated such differentiation by promoting the conjugation of ubiquitin to Foxo1 and subsequent degradation of Foxo1. Given that published studies have shown that Itch has a negative role in regulating the differentiation of T_H2 cells and inflammatory signaling, we propose that Itch is a key participant in the control of both T_H2 cell–mediated allergic inflammation and T_{FH} cell–promoted B cell immunity. Understanding how Itch regulates such different processes may be useful in both rational vaccine design for human infectious diseases and therapeutic intervention in human inflammatory diseases.

METHODS

Methods and any associated references are available in the online version of the paper.

Note: Any Supplementary Information and Source Data files are available in the online version of the paper.

ACKNOWLEDGMENTS

We thank R.A. DePinho (The University of Texas MD Anderson Cancer Center) for *Foxo1*$^{fl/fl}$ and *Foxo3a*$^{fl/fl}$ mice, and members of Liu and Crotty laboratories for advice and help. Supported by the National Institute of Allergy and Infectious Diseases of the US National Institutes of Health (RO1AI062969 and RO1AI078272 to Y.-C.L.; and RO1AI072543 and RO1AI063107 to S.C.).

AUTHOR CONTRIBUTIONS

N.X. designed and executed the experiments, analyzed the data and wrote the manuscript; D.E. helped set up the infection models and the data analysis; C.E. prepared the reagents and maintained mouse breeding colonies; G.P. helped the biochemical experiments; S.C. designed the experiments, helped with the data analysis and wrote the paper; Y.-C.L. initiated and secured funding for the project and helped with data analysis and manuscript preparation.

COMPETING FINANCIAL INTERESTS

The authors declare no competing financial interests.

1. Crotty, S. Follicular helper CD4 T cells (TFH). *Annu. Rev. Immunol.* **29**, 621–663 (2011).
2. Vinuesa, C.G. & Cyster, J.G. How T cells earn the follicular rite of passage. *Immunity* **35**, 671–680 (2011).
3. Victora, G.D. & Nussenzweig, M.C. Germinal centers. *Annu. Rev. Immunol.* **30**, 429–457 (2012).
4. Johnston, R.J. *et al.* Bcl6 and Blimp-1 are reciprocal and antagonistic regulators of T follicular helper cell differentiation. *Science* **325**, 1006–1010 (2009).
5. Nurieva, R.I. *et al.* Bcl6 mediates the development of T follicular helper cells. *Science* **325**, 1001–1005 (2009).
6. Yu, D. *et al.* The transcriptional repressor Bcl-6 directs T follicular helper cell lineage commitment. *Immunity* **31**, 457–468 (2009).
7. Harker, J.A., Lewis, G.M., Mack, L. & Zuniga, E.I. Late interleukin-6 escalates T follicular helper cell responses and controls a chronic viral infection. *Science* **334**, 825–829 (2011).
8. Karnowski, A. *et al.* B and T cells collaborate in antiviral responses via IL-6, IL-21, and transcriptional activator and coactivator, Oct2 and OBF-1. *J. Exp. Med.* **209**, 2049–2064 (2012).
9. Vogelzang, A. *et al.* A fundamental role for interleukin-21 in the generation of T follicular helper cells. *Immunity* **29**, 127–137 (2008).
10. Eto, D. *et al.* IL-21 and IL-6 are critical for different aspects of B cell immunity and redundantly induce optimal follicular helper CD4 T cell (Tfh) differentiation. *PLoS ONE* **6**, e17739 (2011).
11. Nurieva, R.I. *et al.* Generation of T follicular helper cells is mediated by interleukin-21 but independent of T helper 1, 2, or 17 cell lineages. *Immunity* **29**, 138–149 (2008).
12. Choi, Y.S., Eto, D., Yang, J.A., Lao, C. & Crotty, S. Cutting edge: STAT1 is required for IL-6-mediated Bcl6 induction for early follicular helper cell differentiation. *J. Immunol.* **190**, 3049–3053 (2013).

13. Bauquet, A.T. *et al.* The costimulatory molecule ICOS regulates the expression of c-Maf and IL-21 in the development of follicular T helper cells and T_H-17 cells. *Nat. Immunol.* **10**, 167–175 (2009).
14. Choi, Y.S. *et al.* ICOS receptor instructs T follicular helper cell versus effector cell differentiation via induction of the transcriptional repressor Bcl6. *Immunity* **34**, 932–946 (2011).
15. Xu, H. *et al.* Follicular T-helper cell recruitment governed by bystander B cells and ICOS-driven motility. *Nature* **496**, 523–527 (2013).
16. Johnston, R.J., Choi, Y.S., Diamond, J.A., Yang, J.A. & Crotty, S. STAT5 is a potent negative regulator of T_{FH} cell differentiation. *J. Exp. Med.* **209**, 243–250 (2012).
17. Ballesteros-Tato, A. *et al.* Interleukin-2 inhibits germinal center formation by limiting T follicular helper cell differentiation. *Immunity* **36**, 847–856 (2012).
18. Oestreich, K.J., Mohn, S.E. & Weinmann, A.S. Molecular mechanisms that control the expression and activity of Bcl-6 in T_H1 cells to regulate flexibility with a T_{FH}-like gene profile. *Nat. Immunol.* **13**, 405–411 (2012).
19. Choi, Y.S., Yang, J.A. & Crotty, S. Dynamic regulation of Bcl6 in follicular helper CD4 T (Tfh) cells. *Curr. Opin. Immunol.* **25**, 366–372 (2013).
20. Ise, W. *et al.* The transcription factor BATF controls the global regulators of class-switch recombination in both B cells and T cells. *Nat. Immunol.* **12**, 536–543 (2011).
21. Bollig, N. *et al.* Transcription factor IRF4 determines germinal center formation through follicular T-helper cell differentiation. *Proc. Natl. Acad. Sci. USA* **109**, 8664–8669 (2012).
22. Kroenke, M.A. *et al.* Bcl6 and Maf cooperate to instruct human follicular helper CD4 T cell differentiation. *J. Immunol.* **188**, 3734–3744 (2012).
23. Kerscher, O., Felberbaum, R. & Hochstrasser, M. Modification of proteins by ubiquitin and ubiquitin-like proteins. *Annu. Rev. Cell Dev. Biol.* **22**, 159–180 (2006).
24. Huang, H. *et al.* K33-linked polyubiquitination of T cell receptor-ζ regulates proteolysis-independent T cell signaling. *Immunity* **33**, 60–70 (2010).
25. Heissmeyer, V. *et al.* Calcineurin imposes T cell unresponsiveness through targeted proteolysis of signaling proteins. *Nat. Immunol.* **5**, 255–265 (2004).
26. Fang, D. *et al.* Dysregulation of T lymphocyte function in itchy mice: a role for Itch in T_H2 differentiation. *Nat. Immunol.* **3**, 281–287 (2002).
27. Harada, Y. *et al.* Transcription factors Foxo3a and Foxo1 couple the E3 ligase Cbl-b to the induction of Foxp3 expression in induced regulatory T cells. *J. Exp. Med.* **207**, 1381–1391 (2010).
28. Liu, Y.C. Ubiquitin ligases and the immune response. *Annu. Rev. Immunol.* **22**, 81–127 (2004).
29. Perry, W.L. *et al.* The itchy locus encodes a novel ubiquitin protein ligase that is disrupted in a18H mice. *Nat. Genet.* **18**, 143–146 (1998).
30. Jin, H.S. et al. Itch expression by Treg cells controls Th2 inflammatory responses. *J. Clin. Invest.* **123**, 4923–4934 (2013).
31. Oxenius, A., Bachmann, M.F., Zinkernagel, R.M. & Hengartner, H. Virus-specific MHC-class II-restricted TCR-transgenic mice: effects on humoral and cellular immune responses after viral infection. *Eur. J. Immunol.* **28**, 390–400 (1998).
32. Yusuf, I. *et al.* Germinal center T follicular helper cell IL-4 production is dependent on signaling lymphocytic activation molecule receptor (CD150). *J. Immunol.* **185**, 190–202 (2010).
33. Liang, H.E. *et al.* Divergent expression patterns of IL-4 and IL-13 define unique functions in allergic immunity. *Nat. Immunol.* **13**, 58–66 (2012).
34. Kopf, M., Le Gros, G., Coyle, A.J., Kosco-Vilbois, M. & Brombacher, F. Immune responses of IL-4, IL-5, IL-6 deficient mice. *Immunol. Rev.* **148**, 45–69 (1995).
35. Grusby, M.J. Stat4- and Stat6-deficient mice as models for manipulating T helper cell responses. *Biochem. Soc. Trans.* **25**, 359–360 (1997).
36. Hedrick, S.M., Hess Michelini, R., Doedens, A.L., Goldrath, A.W. & Stone, E.L. FOXO transcription factors throughout T cell biology. *Nat. Rev. Immunol.* **12**, 649–661 (2012).
37. Matsuzaki, H., Daitoku, H., Hatta, M., Tanaka, K. & Fukamizu, A. Insulin-induced phosphorylation of FKHR (Foxo1) targets to proteasomal degradation. *Proc. Natl. Acad. Sci. USA* **100**, 11285–11290 (2003).
38. Huang, H. *et al.* Skp2 inhibits FOXO1 in tumor suppression through ubiquitin-mediated degradation. *Proc. Natl. Acad. Sci. USA* **102**, 1649–1654 (2005).
39. Kerdiles, Y.M. *et al.* Foxo transcription factors control regulatory T cell development and function. *Immunity* **33**, 890–904 (2010).
40. Gigoux, M. *et al.* Inducible costimulator promotes helper T-cell differentiation through phosphoinositide 3-kinase. *Proc. Natl. Acad. Sci. USA* **106**, 20371–20376 (2009).
41. Kerdiles, Y.M. *et al.* Foxo1 links homing and survival of naive T cells by regulating L-selectin, CCR7 and interleukin 7 receptor. *Nat. Immunol.* **10**, 176–184 (2009).
42. Ouyang, W. *et al.* Novel Foxo1-dependent transcriptional programs control T_{reg} cell function. *Nature* **491**, 554–559 (2012).
43. Hustad, C.M. *et al.* Molecular genetic characterization of six recessive viable alleles of the mouse agouti locus. *Genetics* **140**, 255–265 (1995).
44. Huang, H. & Tindall, D.J. Regulation of FOXO protein stability via ubiquitination and proteasome degradation. *Biochim. Biophys. Acta* **1813**, 1961–1964 (2011).
45. Ouyang, W. *et al.* Foxo proteins cooperatively control the differentiation of $Foxp3^+$ regulatory T cells. *Nat. Immunol.* **11**, 618–627 (2010).
46. Fernández de Mattos, S. *et al.* FoxO3a and BCR-ABL regulate cyclin D2 transcription through a STAT5/BCL6-dependent mechanism. *Mol. Cell. Biol.* **24**, 10058–10071 (2004).
47. Baumjohann, D. *et al.* The microRNA cluster miR-17 approximately 92 promotes T_{FH} cell differentiation and represses subset-inappropriate gene expression. *Nat. Immunol.* **14**, 840–848 (2013).
48. Kang, S.G. *et al.* MicroRNAs of the miR-17 approximately 92 family are critical regulators of T_{FH} differentiation. *Nat. Immunol.* **14**, 849–857 (2013).

ONLINE METHODS

Mice. *Itch*$^{-/-}$ mice on a C57BL/6J (B6) background have been described[26]. Heterozygous *Itch*$^{+/-}$ mice were intercrossed to generate *Itch*$^{+/+}$, *Itch*$^{+/-}$ and *Itch*$^{-/-}$ littermates. *Itch*$^{fl/fl}$ mice on the B6 background have been described[30]. SMARTA mice (with transgenic expression of a T cell antigen receptor specific for the epitope of LCMV glycoprotein amino acids 66–77 presented by I-A^{b}) were fully backcrossed to the B6 background[31]. *Itch*$^{-/-}$ SMARTA mice were generated by the crossing of wild-type SMARTA to *Itch*$^{-/-}$ mice. *Il4*$^{-/-}$, CD4-Cre and Mx1-Cre mice were from the Jackson Laboratory. *Foxo1*$^{fl/fl}$ and *Foxo3a*$^{fl/fl}$ mice on the 129 background were provided by R.A. DePinho and were bred onto the B6 background for six generations. All animal protocols were approved by members of the Institutional Animal Care and Use Committee of the La Jolla Institute for Allergy and Immunology.

Antibodies and reagents. Anti-CD4 (GK1.5 and RM4-5), anti-CD25 (PC61.5), anti-CD44 (IM7), anti-CD45.1 (A20), anti-CD45.2 (104), anti-ICOS (15F9), anti-IgD (11-26) and streptavidin were from eBioscience. Anti-B220 (RA3-6B2), anti-CD62L (MEL-14), anti-CD69 (H1.2F3), anti-CD150 (anti-SLAM; TC15-12F12.2), anti-interferon-γ (XMG1.2) anti-ICOS purified to be low endotoxin and azide free (used for *in vitro* stimulation; C398.4A) and anti-CD3 (2C11) were from Biolegend. Anti-CD8α (53-6.7), anti-CD95 (FAS, Jo2), anti-CD138 (281-2), anti-PD-1 (J43), anti-CXCR5 (2G8), biotin-conjugated anti-CXCR5 (2G8), anti-Bcl-6 (K112-91), anti-CD95 (Jo2), antibody to the T cell– and B cell–activation antigen (GL7) and anti-IL-4 (BVD4-1D11) were from BD Pharmingen. Anti-Itch (32/Itch) was from BD Transduction Laboratories. Antibody to Akt phosphorylated at Ser473 (D9E) or Thr308 (244F9), anti-Foxo1 (L27 and C29H4) and antibody to Foxo1 phosphorylated at Ser256 (9461) were from Cell Signaling Technology. Anti-Foxo1 (ab39670) was from Abcam. Anti-Myc (9E10), anti-actin (C4) and anti-ubiquitin (P4D1) were from Santa Cruz. Purified anti-CD28 (37.51) was from Bio-X-Cell. Purified antibody to Armenian hamster IgG (127-005-099) and biotin–conjugated goat antibody to rat IgG (112-065-167) were from Jackson ImmunoResearch. Polyclonal antibody to ubiquitin was raised in a rabbit immunized with ubiquitin peptide, in collaboration with Millipore. Recombinant human IL-2 and mouse IL-7 were from Peprotech.

Plasmids and cell transfection. cDNA encoding Itch or hemagglutinin-tagged ubiquitin has been described[26]. cDNA encoding Foxo1 or Foxo3a (Addgene) was subcloned into plasmid pEF4mychisB. For the construction of shRNA expression vectors, oligonucleotides were cloned into the vector pLMP-Ametrine.

For protein expression in Jurkat T cells, cells were transfected with the appropriate amount of plasmid (5–20 μg) by electroporation (260 V and 950 μF; Bio-Rad). Cells were lysed for 30 min on ice in NP-40 lysis buffer (1% NP-40, 20 mM Tris-HCl, pH 7.5, 150 mM NaCl, 5 mM EDTA, 5 mM NaPiP, 5 mM NaF, 2 mM Na_3VO_4 and 10 μg/ml each of aprotinin and leupeptin) and cell debris were removed by centrifugation at 13,200 r.p.m. for 10 min at 4 °C.

Retroviral transduction and cell transfer. shRNA-containing oligonucleotides (**Supplementary Table 1**) were cloned into the plasmid pLMPd-Ametrine. Plat-E packaging cells were transfected with 3 μg of retroviral vector (pMIG-GFP or pMIG–Bcl-6 (ref. 4), or pLMPd-Ametrine) along with 9 μl of TransIT-LT1 transfection reagent (Mirus). 48 h after transfection, the culture supernatant containing retrovirus was collected. Naive CD4^{+}CD44^{-}CD62L^{+}CD25^{-} T cells were stimulated with plate-bound anti-CD3 (2C11; Biolegend) and anti-CD28 (37.51; Bio-X-Cell). 24 h after stimulation, CD4^{+} T cells were infected with retrovirus together with 10 μg/ml polybrene and 100 U/ml IL-2 by centrifugation of cells at 2,000 r.p.m. for 60 min at room temperature. A second transduction was repeated 24 h after the first transduction. 24 h after the second transduction, cells were transferred to fresh medium with 100 U/ml IL-2, followed by incubation for 2 d. Cells were then transferred to new medium with 1 ng/ml IL-7, followed by incubation for 24 h before being sorted. Naive or retrovirus-transduced SMARTA CD4^{+} T cells were transferred into recipient mice by intravenous injection into the retro-orbital sinus. Naive SMARTA CD4^{+} T cells were transferred for experiments on day 3 (5×10^5 cells) and day 8 (2.5×10^3 cells). 5×10^5 or 2.5×10^4 retrovirus-transduced SMARTA CD4^{+} T cells were transferred for experiments at day 3 or day 8, respectively.

Bone marrow chimeras with knockdown by shRNA. For the generation of chimeric mice expressing shRNA, Plat-E cells were transfected with 3 μg of pLMPd-Ametrine vector through the use of 9 μl of TransIT-LT1 (Mirus). 48 h after transfection, the culture supernatant containing retrovirus was collected. SMARTA (CD45.1^{+}) bone marrow depleted of mature T cells was cultured for 24 h in complete DMEM containing 10 ng/ml IL-3, 10 ng/ml IL-6, and 100 ng/ml stem cell factor (all from Peprotech) before initial retroviral infection. Bone marrow depleted of mature T cells as infected with retrovirus along with 5 μg/ml polybrene (Sigma-Aldrich) by centrifugation (2,000 r.p.m. for 1 h). 24 h after infection, retrovirus-transduced bone marrow cells were injected into lethally irradiated (900 rads) B6 recipient mice.

Infection. Stocks of VACV (Western Reserve strain) and LCMV (Armstrong strain) were prepared and 'titrated' as described[49]. Virus was prepared in plain DMEM. Each mouse was infected with 5×10^5 or 1×10^5 plaque-forming units of LCMV (Armstrong strain) for experiments at day 3 or day 8, respectively, by bilateral intraperitoneal injection. Each mouse was infected with 2.5×10^5 VACV (Western Reserve strain) by bilateral intraperitoneal injection.

Neutralization of IL-2 *in vivo*. Anti-IL-2 (S4B6) and isotype-matched control antibody (rat IgG2a; 2A3) were from Bio-X-Cell. Each B6 mouse was treated with 0.5 mg anti-IL-2 or isotype-matched control antibody by both intraperitoneal and retro-orbital injection 24 h before infection with LCMV and then again 24 h after infection with LCMV.

Inducible deletion of Itch and/or Foxo1. For inducible deletion of Itch and/or Foxo1, *Itch*$^{fl/fl}$ and/or *Foxo1*$^{fl/fl}$ mice were crossed with mice expressing Cre recombinase under control of the interferon-responsive *Mx1* promoter (Mx1-Cre). For activation of the interferon-inducible Mx1-Cre, 6-week-old mice were injected intraperitoneally with 250 μl of 1 mg/ml poly(I:C) every the other day for a total of three injections. All mice were infected with VACV 2 weeks after the final poly(I:C) treatment.

ELISA. Concentrations of cytokines in serum were measured by sandwich ELISA according to the instructions from Biolegend. Anti-VACV IgG was quantified by ELISA in lysates of cells infected with VACV that had been inactivated by ultraviolet irradiation as the capture antigen. 96-well PolySorp microtiter plates (Nunc) were coated overnight lysates of cells infected with VACV inactivated by ultraviolet irradiation, in PBS. After incubation of sample serum, plates were incubated with biotin-conjugated goat antibody to mouse IgG (1030-08; Southern Biotech), followed by horseradish peroxidase–conjugated streptavidin (7100-05; Southern Biotech) and then tetramethylbenzidine substrate solution (172-1068; Bio-Rad).

Real-time quantitative PCR. Total RNA was extracted with an RNeasy mini or RNeasy plus micro kit (Qiagen). cDNA was synthesized with SuperScript III Reverse Transcriptase (Invitrogen) and oligo(dT). Quantitative PCR was done in duplicate with iTaq Universal SYBR Green Supermix (Bio-Rad) on a Roche LightCycler 480 (Roche). β-actin was used as the reference for normalization. Primers for Itch (QT01048684) were from Qiagen; all other primers are in **Supplementary Table 2**.

Immunoprecipitation, glutathione *S*-transferase precipitation assay and immunoblot analysis. Proteins were immunoprecipitated by incubation of the cell lysates overnight at 4 °C with the appropriate antibodies (1 μg; all identified above), followed by the addition of protein A/G–Magnetic beads (88802; Thermo Scientific) and incubation for another 2 h at 4 °C. Immunoprecipitates were washed five times with NP-40 lysis buffer and were boiled in 50 μl SDS loading buffer. For endogenous coimmunoprecipitation, a combination of cytosolic and nuclear fractions from primary CD4^{+} T cells was incubated with anti-Foxo1 (ab39670; Abcam). For glutathione *S*-transferase (GST) precipitation assays, a GST fusion protein or GST alone (5 μg) was added to lysates of Jurkat cells, followed by incubation for 2 h at 4 °C, then 50 μl of glutathione-Sepharose beads (17-0756-01; GE Healthcare) was added,

followed by incubation for another 1 h. Precipitates were washed five times with NP-40 lysis buffer and were boiled in 50 µl SDS loading buffer. For visualization of ubiquitinated protein, 1.0% SDS was added to lysis buffer for disruption of nonspecific protein interactions. Cell lysates were denatured by being boiled for 15 min and then were diluted to a concentration of 0.1% SDS before immunoprecipitation. Samples were separated to 10–12% SDS-PAGE, followed by electrotransfer to PVDF membranes (Millipore). Membranes were analyzed by immunoblot with the appropriate antibodies (all identified above), followed by horseradish peroxidase-conjugated second antibody (NA931V or NA934V; GE Healthcare) and development with an enhanced chemiluminescence detection system (RPN2106, RPN2232 or RPN2235; GE Healthcare).

T cell–restimulation assay. Primary T cells were cultured in RPMI-1640 medium supplemented with 10% FBS, glutamine, HEPES (10 mM), sodium pyruvate (1 mM), β-mercaptoethanol, penicillin and streptomycin. Primary $CD4^+$ T cells were isolated from spleens and lymph nodes of 2- to 3-month-old wild-type and *Itch*$^{-/-}$ mice with a negative selection kit from BD. For the preparation of $CD4^+$ T cell blasts, T cells were activated for 2 d by plate-bound anti-CD3 (3 µg/ml) and anti-CD28 (3 µg/ml) (both identified above) and were allowed to 'rest' for 1 d in medium alone. The $CD4^+$ T cell blasts were harvested and then were restimulated by combinations of anti-CD3 (3 µg/ml) and anti-ICOS (2 µg/ml) (both identified above). The antibodies were crosslinked at 37 °C by goat antibody to hamster IgG (20 µg/ml; identified above) and the cells were restimulated for various times. After being restimulated, cells were lysed for 20 min in 2× SDS loading buffer and were boiled for 10 min. Cell lysates were then subjected to immunoblot analysis with the appropriate antibodies (all identified above).

Flow cytometry. Single-cell suspensions of splenocytes were prepared by mashing of spleens through a cell strainer. After treatment with red-blood-cell–lysis buffer, surfaces of cells in suspension were stained with fluorochrome-conjugated antibodies (all identified above) in flow cytometry buffer (0.5% BSA and 0.05% NaN_3 in PBS). For experiments at day 8 of infection with VACV, a three-step CXCR5 staining was performed with purified anti-CXCR5 (2G8; BD PharMingen), followed by biotinylated goat antibody to rat IgG (112-065-167; Jackson ImmunoResearch) and then phycoerythrin-indotricarbocyanine–labeled streptavidin (25-4317-82; eBioscience), with each staining step done at 4 °C in CXCR5 staining buffer (0.5% BSA, 2% FCS and 2% normal mouse serum in PBS). For adoptive transfer experiments with LCMV infection, a two-step CXCR5 staining was performed with biotinylated anti-CXCR5 (2G8, BD PharMingen), followed by phycoerythrin–indotricarbocyanine–labeled streptavidin.

Intracellular cytokines were stained after stimulation of cells for 4 h with 50 ng/ml PMA (phorbol 12-myristate 13-acetate; Sigma-Aldrich) and 1 µg/ml ionomycin (Sigma-Aldrich) in the presence of GolgiStop. Cells were incubated with antibodies to cell surface markers (all identified above), and then were fixed and permeabilized with Cytofix/Cytoperm Buffer (51-2090KZ; BD Biosciences). Cells were then stained with antibodies to cytokines (all identified above). Intracellular Bcl-6 (K112-91; BD Bioscience) was stained after cell-surface staining. Samples were fixed and permeabilized with Foxp3 staining buffer according to the manufacturer's manual (00-5523 ; eBioscience). Samples were incubated for 45–60 min at 4 °C with Fixation/Permeabilization buffer and washed with 1× permeabilization buffer. Samples were incubated for another 45–60 min with Alexa Fluor 647–conjugated monoclonal antibody to Bcl-6 (identified above) in permeabilization buffer.

Statistical analysis. All data were analyzed by a paired or unpaired *t*-test with GraphPad Prism 5.0.

49. McCausland, M.M. *et al*. SAP regulation of follicular helper CD4 T cell development and humoral immunity is independent of SLAM and Fyn kinase. *J. Immunol.* **178**, 817–828 (2007).

doi:10.1038/ni.2912